Egypt. J. Chem. **Vol. 67**, No. 11 pp. 277 -288 (2024)

Egyptian Journal of Chemistry

http://ejchem.journals.ekb.eg/

Steel corrosion resistance with new 2-mercaptopyrimidin-4-ol derivatives

Adel A. H. Abdel-Rahman[1*], Aly Abdelmaboud[2] and Asmaa Said Hassan[1]

[1]*Department of Chemistry, Faculty of Science, Menoufia University, Shebin El-Koam, Egypt*

[2] *Department of Chemistry, Faculty of Science, Benha University, Egypt*

Abstract

Three six-amino pyrimidine derivative chemicals were recently identified; ***P(3)***, *2-mercaptopyrimidin-4-ol*, ***P(5)***, *(E)-6-(benzylideneamino)-2-mercaptopyrimidin-4-ol*, and ***P(6)***, *(E)-Ethyl-2-{[(4-(benzylideneamino)-6-hydroxypyrimidin-2yl) thio]}acetate*. FTIR and ^{1}H NMR provided confirmation of the synthesized substance's chemical structure. The newly synthesized cationic pyrimidine derivatives were investigated for their potential as carbon steel corrosion inhibitors in acidic solutions via impedance and potentio-dynamic polarization spectra. The inhibitory efficiencies derived from the several methods used are largely in line with one another. The Tefel findings demonstrated that the compounds effectively prevented carbon steel from corroding under the examined corrosive conditions, with an inhibition efficacy of 78.21, 78.74 and 81.37%, for ***P(3)***, ***P(5)*** and ***P(6)***, respectively. Using the Frumkin isotherm, it was determined that these chemicals' inhibitory impact was related to their adsorption on carbon steel surface. The surface of the carbon steel was inspected with SEM.

Keywords: Corrosion inhibitors, Carbon steel, Pyrimidine derivatives, Potentiodynamic polarization and Electrochemical impedance.

1. Introduction

Pyrimidine is a π-deficient heterocycle. Due to its lower electron densities, the 2, 4, and 6 locations are extremely electrophilic. Also, it retains its benzenoid characteristics sometimes at 5 location [1,2]. Tautomerism of heterocycles with six members like pyrimidines, has been extensively studied in recent years [3]. Analyses of the interactions between annular nitrogens and electrophiles have been reported [4]. The pyrimidinones are changed into the appropriate silyl ethers before being N-alkylated [5].

Corrosion inhibitors are commonly employed to suppress or at least moderate the corrosion process of metals in a variety of industries, from construction materials to surface treatments for cultural artifacts [6-7]. Most of the inhibitors that form protective barriers against adsorption are organic. Often, they feature a surfactant-containing molecular structure with a hydrophilic group that can stick to the metal surface and a hydrophobic part that penetrates the majority of the fluid. Adsorbed inhibitor molecules stop

*Corresponding author e-mail: adelnassar63@yahoo.com.;(Adel A. H. Abdel-Rahman).
EJCHEM use only: Received date 08 August 2024; revised date 11 September 2024; accepted date 28 September 2024
DOI: 10.21608/ejchem.2024.310848.10163

oxygen and water from accessing the metal surface, thereby slowing down the rate of corrosion. [8]. It has been found that at concentrations that successfully prevent copper metal from corroding in acidic settings, heterocyclic pyrimidine is a safe inhibitor. Several pyrimidine derivatives were employed as steel corrosion inhibitors in HCl and H_2SO_4 solutions based on their percentage inhibition (% IE). Two nitrogen atoms can be found in positions one and three of the aromatic heterocyclic compound pyrimidine's six-member ring. Several pyrimidine derivatives have biological and pharmacological properties such as anticonvulsant, antibacterial, antifungal,, antiviral, and anticancer activities [9–10]. Nowadays, pyrimidine derivatives are regarded as environmentally benign compounds due to their diverse biological activity. Pyrimidine molecules also fit the description of an organic material that is an effective corrosion inhibitor: they are able to transfer electrons to the empty metal surface d-orbital forming coordinates, and also deliver electrons to their anti-bonding orbitals forming feedback bonds. Pyrimidine compounds are therefore expected to be effective corrosion inhibitors for their low toxicity and efficacy [10]. Organic corrosion inhibitors are less harmful to the environment than their inorganic counterparts, with a few notable exceptions [11–13]. Among these chemical substances are pyridine, imidazole, triazine, and indole. These organic molecules mix with the steel to create a covering that protects it from the corrosive acid solution [14–15]. Pyrimidines have been demonstrated to be ecologically friendly organic corrosion inhibitors in acidic settings. Pyrimidines are rarely utilized in industry, despite their remarkable capacity to inhibit corrosion [16–17]. The goal of the current work was to synthesize new pyrimidine derivatives and comprehensively assess their capacity to lessen carbon steel corrosion in 1M HCl, keeping in mind the previously mentioned aspects. ***P(5)***, *(E)-6-(benzylideneamino)-2-mercaptopyrimidin-4-ol*, ***P(6)***, *ethyl-2-{[(4-(benzylideneamino)-6-hydroxypyrimidin-2yl)thio]}acetate*, and ***P(3)***, *6-Amino-2-mercaptopyrimidin-4-ol* are the produced compounds. The investigation's different corrosion mitigation capabilities are discussed in detail.

2. Experimental

2.1. Chemicals

The used carbon steel for investigation has the following composition:

Table 1: Structure of the carbon steel utilized in the study is as follows:

Element	C	Si	P	Mn	Cr	V	S	Fe
Content %	0.13	0.35	0.06	0.50	2.28	0.24	0.002	> 96

The chemicals used in the investigation are sodium metal, ethanol and thiourea from Aldrich, St. Louis, USA, ethyl carbonocyanidate, para hydroxybenzaldhyde, hydrazine hydrate, 6-amino-2-mercaptopyrimidin-4-ol and ethyl chloro acetate from POCH SA, Gliwice, Poland, acetic acid and benzoic acid from Loba Chemie, Colaba, Mumbai, India, ortho hydroxy benzaldhyde and phthalic anhydride from Acros Organics, Antwerp, Belgium, succinic acid and butanol from Merck-Schuchardt, Hohenbrunn, Germany.

2.2. Synthesis of nitrogen heterocyclic compounds

2.2.1. Synthesis of *6-Amino-2-mercaptopyrimidin-4-ol: P(3)*

First, ethanol (30 mL) was used to dissolve sodium metal (0.1 M). The 0.1 M thiourea, dissolved in ethyl cyano acetate was added and the mixture was refluxed for 25 hours, then filtered, concentrated, and recrystallized by ethanol. The yield is *6-amino-2-mercaptopyrimidin-4-ol*, ***P(3)***: (83%) as a yellow solid with M.P. 120–130 °C, **Scheme 1.**

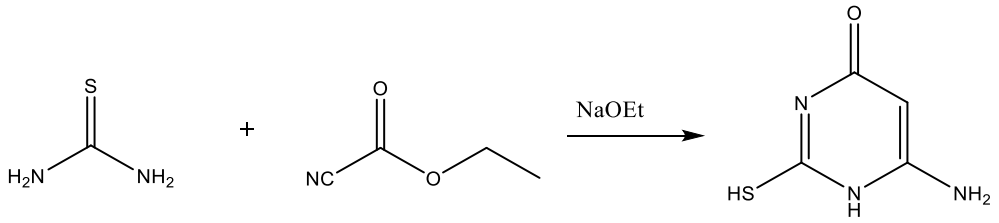

(2) **(3)**

Scheme 1

2.2.2. Synthesis of *(E)-6-(benzylideneamino)-2-mercaptopyrimidin-4-ol: P(5)*

6-amino-2-mercaptopyrimidin-4-ol (1g) is added to 1g of p.hydroxybenzaldehyde, dissolved in ethanol and refluxed for 4h, concentrated, filtered, and recrystallized using ethanol. The yield is *(E)-6-(Benzylideneamino)-2-mercaptopyrimidin-4-ol*, ***P(5)***: (85%) as a yellow solid; M.P. 130-150 ^{0}C, **Scheme 2**.

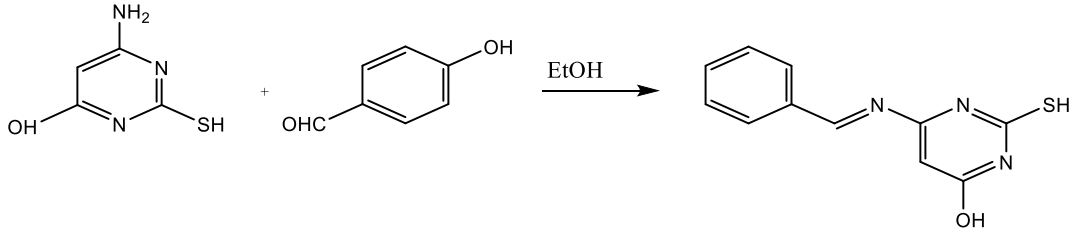

(3) **(4)** **(5)**

Scheme 2

2.2.3. Synthesis of *ethyl-2-{[(4-(benzylideneamino)-6-hydroxypyrimidin-2-yl)thio]}acetate: P(6)*

(E)-6-(Benzylideneamino)-2-mercaptopyrimidin-4-ol (6mmol) is added to 50 mL ethyl chloro acetate/ethanol solution, refluxed for 8h, concentrated, filtered and recrystallized using ethanol to produce the third yield; *ethyl-2-{[(4-(benzylideneamino)-6-hydroxypyrimidin-2-yl)thio]}acetate*, ***P(6)*****:** (85%) as a yellow solid; M.P. 150-180 ^{0}C, **Scheme 3**.

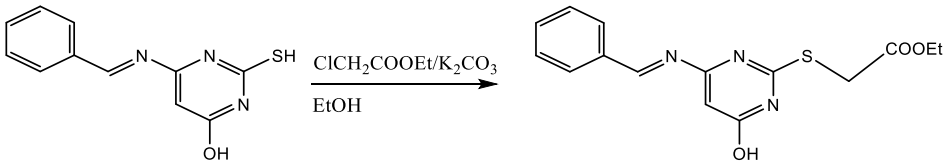

(5) **(6)**

Scheme 3

2.3. Characterization of the synthesized heterocycle compounds

A Thermos Nicolet IS10 FT-IR Spectrophotometer from Thermo Fisher Scientific Inc., Waltham, MA, USA, is used to obtain FT-IR spectra. TLC was used to purify each yield. Nuclear magnetic resonance spectra were recorded using an AVANCE III 400 MHz spectrometer by Bruker, Billerica, MA, USA. The molecules' mass ranged from 39 to 400 a.m.u., and their ionization voltage was 70 eV. Molecule fragments were identified by

Thermo Scientific, USA, Trace GC Ultra/ISQ Single Quadrupole MS, TG-5MS detection.

2.4. Electrochemical techniques

A three-electrode cell; an exposed carbon steel sheet measuring 1.0 cm^2 working electrode, a saturated calomel electrode (SCE) reference, and a platinum auxiliary electrode. Potential was scanned at a rate of 5 mV/s within a (-1.0 to 1.0V) range. A mirror-like gloss was mechanically achieved on the working electrode by using emery sheets with grits of 800, 1000, and 1200. The polished electrode was then fully cleaned using acetone and double-distilled water. Electrochemical software (Nova 1.11) connected the Potentimat/Galvanostat Autolab/PGSTAT204/20 V/400 mA electrochemical measurement instrument to a PC.

2.5. SEM analysis

For one hour, the steel coupons were submerged in 100 mL of the corrosive solution, both with and without the synthetic pyrimidine compounds at a concentration of 10-3 M. After that, they were taken out, rapidly cleaned with acetone, and dried. The specimens' surface morphology was investigated with a JEOL-JSM-6380LA Scanning Electron Microscope.

3. RESULTS AND DISCUSSION

3.1. Structure elucidation

***P(3): 6-Amino-2-mercaptopyrimidin-4-ol* was elucidated by:**

IR (KBr) cm^{-1} ν_{max}: As illustrated in **Figure 1**, the IR spectrum displayed characteristic bands at 3405-3185 (ν_{OH} and ν_{NH2}), 2523 (ν_{SH}), 3055 ($\nu_{CH\ Ar}$), 1544 ($\nu_{C=C\ Ar}$), and 1405 ($\nu_{C=N}$).

***P(5): (E)-6-(benzylideneamino)-2-mercaptopyrimidin-4-ol* was elucidated by:**

IR (KBr) cm^{-1} ν_{max}: As illustrated in **Figure 1**, the IR spectrum displayed characteristic bands at 3407 (ν_{OH}), 2595 (ν_{SH}), 3060 ($\nu_{CH\ Ar}$), 1511 ($\nu_{C=C\ Ar}$), and 1435 ($\nu_{C=N}$).

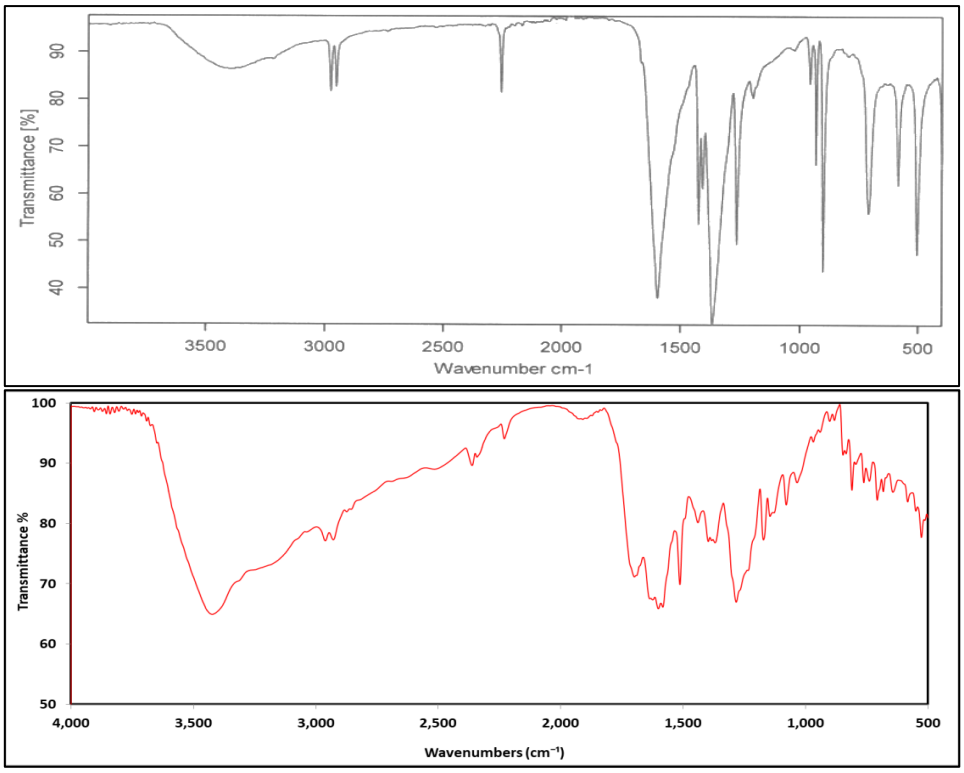

Figure 1: FTIR for **P(3)**: 6-Amino-2-mercaptopyrimidin-4-ol, (above) and **P(5)**: (E)-6-(benzylideneamino)-2-mercaptopyrimidin-4-ol, (below)

***P(6): ethyl-2-{[4-(benzylideneamino)-6-hydroxypyrimidin-2-yl)thio]}acetate* was elucidated by:**

IR (KBr) cm^{-1} ν_{max}: IR spectrum showed characteristic bands at 3410 (ν_{OH}), 3022 (ν_{CH} Ar), 2901 (ν_{CH} Alkane), 1740 ($\nu_{C=O}$), 1544 (ν_{COO}), 1514 ($\nu_{C=C}$ Ar), 1409 ($\nu_{C=N}$), 1288 (ν_{CH3}), 1235 (ν_{CH2}), 730 (ν_{CS}).

^{1}H NMR-400 MHz, δppm (DMSO-d_6): 7.98 (s, 1H), 7.08 (δ, *J* = 11.0 Hz, 1H), 6.99 (δ, *J* = 8.8 Hz, 2H), 6.93 – 6.81 (m, 3H), 5.51 (s, 1H), 4.40 – 4.14 (m, 4H), 1.20 – 0.92 (m, 3H).

EI-MA: m/z ($C_{15}H_{15}N_3O_3S$) calcd = 319 [M^+], shown in **Figure 2**.

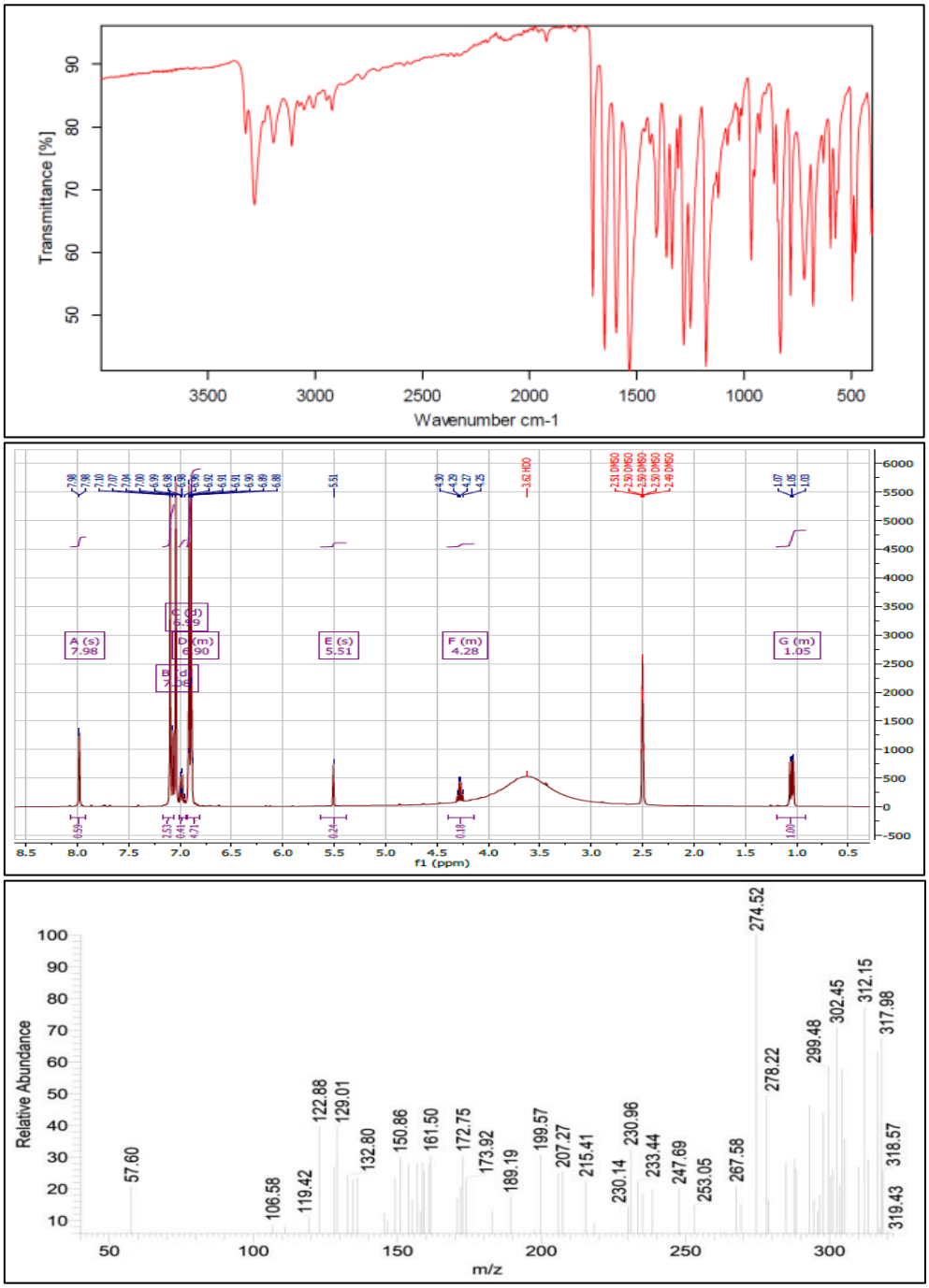

Figure 2: FTIR, ^{1}H NMR and Mass Spectra for **P(6)**: ethyl-2-{[4-(benzylideneamino)-6-hydroxypyrimidin-2-yl)thio]}acetate

3.2. Potentiodynamic polarization

The potentiodynamic polarization curves of carbon steel in 1M HCl solution are shown in **Figure 3**, both uncontrolled and impacted by varying quantities of the pyrimidine derivatives synthesized under investigation. Both surface coverage and inhibitory efficiency were valuated utilizing the subsequent formulas [18]:

$$\%IE = \left(1 - \frac{i_{Pyr}}{i_f}\right) \times 100 \quad (1)$$

$$\theta = \left(1 - \frac{i_{Pyr}}{i_f}\right) \quad (2)$$

i_{Pyr} and i_f, respectively, are the corrosion current densities with and free of the synthesized pyrimidine derivatives being tested. The results show that when the synthesized compounds are added, the cathodic and anodic corrosion current densities significantly drop. This suggests that the molecules of the produced compounds adsorb on both cathodic and anodic metallic surface-active sites through electron-rich heteroatoms and antibonding empty centers, hence impeding the corrosion process.

The values of anodic and cathodic Tafel slopes (β_a and β_c) varied slightly as the concentration of the synthetic compounds under test, was raised. This implies that the mechanisms of carbon steel dissolving and oxygen reduction stay the same upon the modification of both cathodic and anodic processes [19].

These synthetic compounds are considered mixed type inhibitors, meaning they limit both cathodic and anodic processes, because the corrosion potentials (E_{corr}) were nearly unshifted [19–20]. The inhibition efficiencies values increase in the following order, as **Table 2** inspection demonstrates: ***P(3) < P(5) < P(6)***

Table 2: Potentiodynamic polarization parameters for carbon steel in 1M HCl solution and different concentrations of **P(3)**, **P(5)** and **P(6)** at 298 K and scan rate of 5 mV/sec.

Solution	Conc. (M)	β_a (mV/dec)	$-\beta_c$ (mV/dec)	$-E_{corr}$, (mV)	i_{corr} (mA)	θ	Ln[θ/C(1-θ)]	%IE
1M HCl	**Blank**	78	85	408	30.8	-	-	-
P(3)	$\mathbf{1\times10^{-5}}$	87	92	418	26.3	0.15	9.43	14.58
	$\mathbf{1\times10^{-4}}$	80	87	410	20.4	0.34	7.71	33.66
	$\mathbf{5\times10^{-4}}$	84	87	415	15.9	0.48	6.21	48.31
	$\mathbf{1\times10^{-3}}$	82	94	412	6.7	0.78	5.14	78.21
P(5)	$\mathbf{1\times10^{-5}}$	79	91	410	25.7	0.16	9.53	16.49
	$\mathbf{1\times10^{-4}}$	80	92	411	18.1	0.41	7.79	41.13
	$\mathbf{5\times10^{-4}}$	79	89	409	11.3	0.63	6.14	63.23
	$\mathbf{1\times10^{-3}}$	82	93	412	6.5	0.79	5.12	78.74
P(6)	$\mathbf{1\times10^{-5}}$	84	89	415	25.1	0.19	9.63	18.73
	$\mathbf{1\times10^{-4}}$	85	86	415	15.4	0.50	7.82	50.06
	$\mathbf{5\times10^{-4}}$	82	87	413	7.6	0.75	5.92	75.22
	$\mathbf{1\times10^{-3}}$	83	88	413	5.7	0.81	5.02	81.37

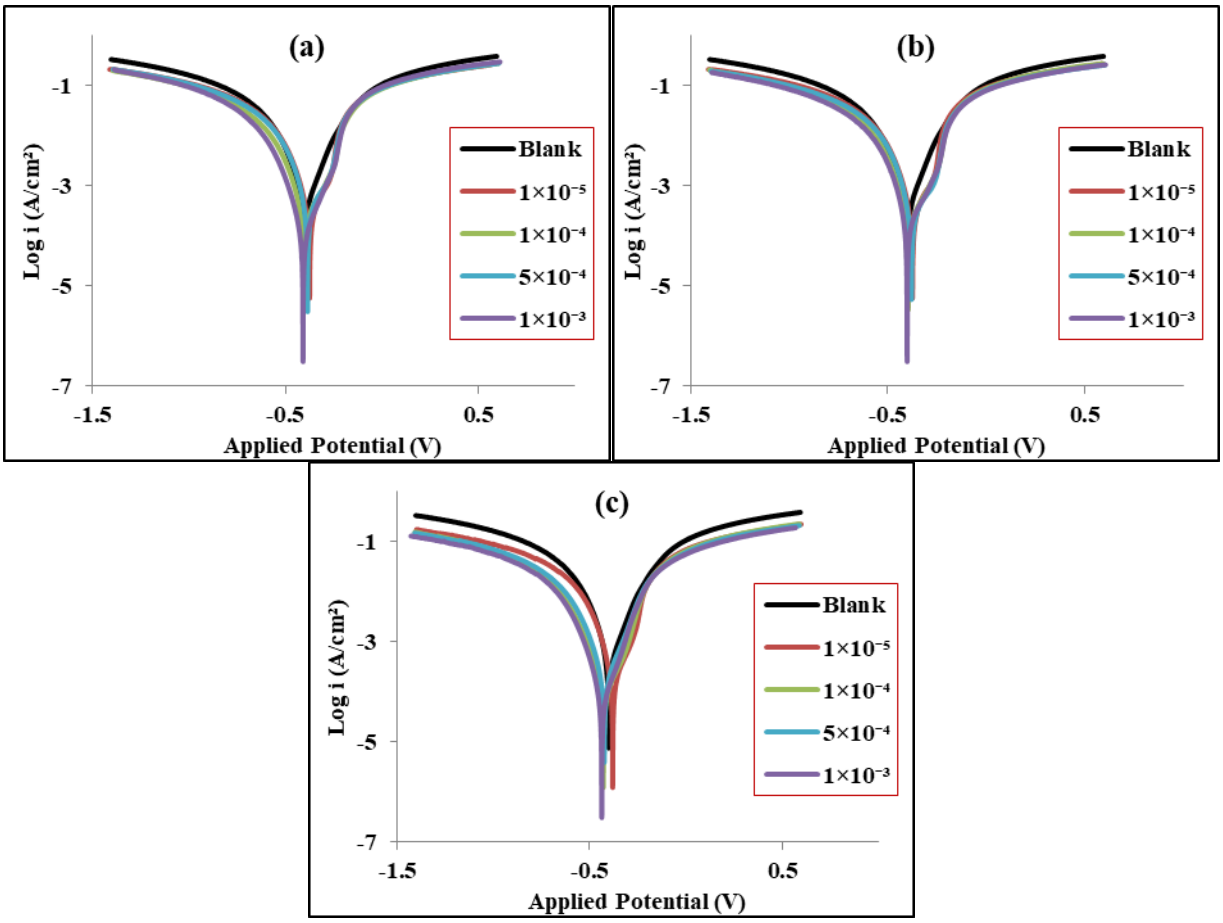

Figure 3: Potentiodynamic polarization curves for carbon steel in 1M HCl solution with different concentrations of a) **P(3)** b) **P(5)** and c) **P(6)** at 298 K and scan rate of 5 mV/sec

3.3. Electrochemical Impedance Spectroscopy

Figure 4 displays the produced Bode diagrams as well as Nyquist plots. Equation [21] can be used to compute the inhibitory efficiency (%IE) of the synthesized pyrimidine derivatives that were tested based on their polarization resistance values.

$$\%IE = \left(1 - \frac{R_{P,f}}{R_{P,Pyr}}\right) \times 100 \qquad (3)$$

where $R_{P,f}$ and $R_{P,Pyr}$ are the polarization resistances in the presence and absence of the tested synthesized pyrimidine derivatives, respectively.

The figures clearly demonstrate an increase in the Nyquist plots diameter, as the concentration of the synthesized compounds increases. The charge transfer and the adsorption of the synthetic substances on the carbon steel surface is the cause, indicating an inhibitory effect of the tested compounds; they cause a lack of the charge transfer process [22].

Table 3: EIS parameters of carbon steel in 1M HCl solution with different concentrations of **P(3)**, **P(5)** and **P(6)** at room temperature.

Solution	Conc. (M)	R_s (Ω)	R_p (Ω)	%IE
1M HCl	**Blank**	2	19	-
P(3)	**1×10^{-5}**	3	48	60.48
	1×10^{-4}	2	52	64.11
	5×10^{-4}	3	61	69.01
	1×10^{-3}	3	103	81.58
P(5)	**1×10^{-5}**	3	60	68.73
	1×10^{-4}	4	86	78.08
	5×10^{-4}	4	108	82.51
	1×10^{-3}	4	128	85.18
P(6)	**1×10^{-5}**	2	62	69.45
	1×10^{-4}	3	83	77.15
	5×10^{-4}	4	134	85.82
	1×10^{-3}	4	203	90.68

Because the molecules of the produced compounds stick to the carbon steel surface, phase angle values increase with increasing

concentrations of the compounds and eventually approach -90°, the ideal value for a capacitor [23]. It's possible that during the adsorption process, the molecules of the generated chemicals smooth down the surface of the carbon steel [24].

Furthermore, the Bode graphs clearly show an increase in impedance values with increasing concentrations of the formed compounds, suggesting that the presence of the produced pyrimidine derivatives significantly inhibits the pace at which carbon steel corrodes [25].

Examining **Figure 4** shows that the produced pyrimidine derivatives concentration has an impact on the inhibition efficiency. Examining **Table 3** shows that the inhibition efficiencies sequence is consistent with that obtained from the results of Tafel measurements.

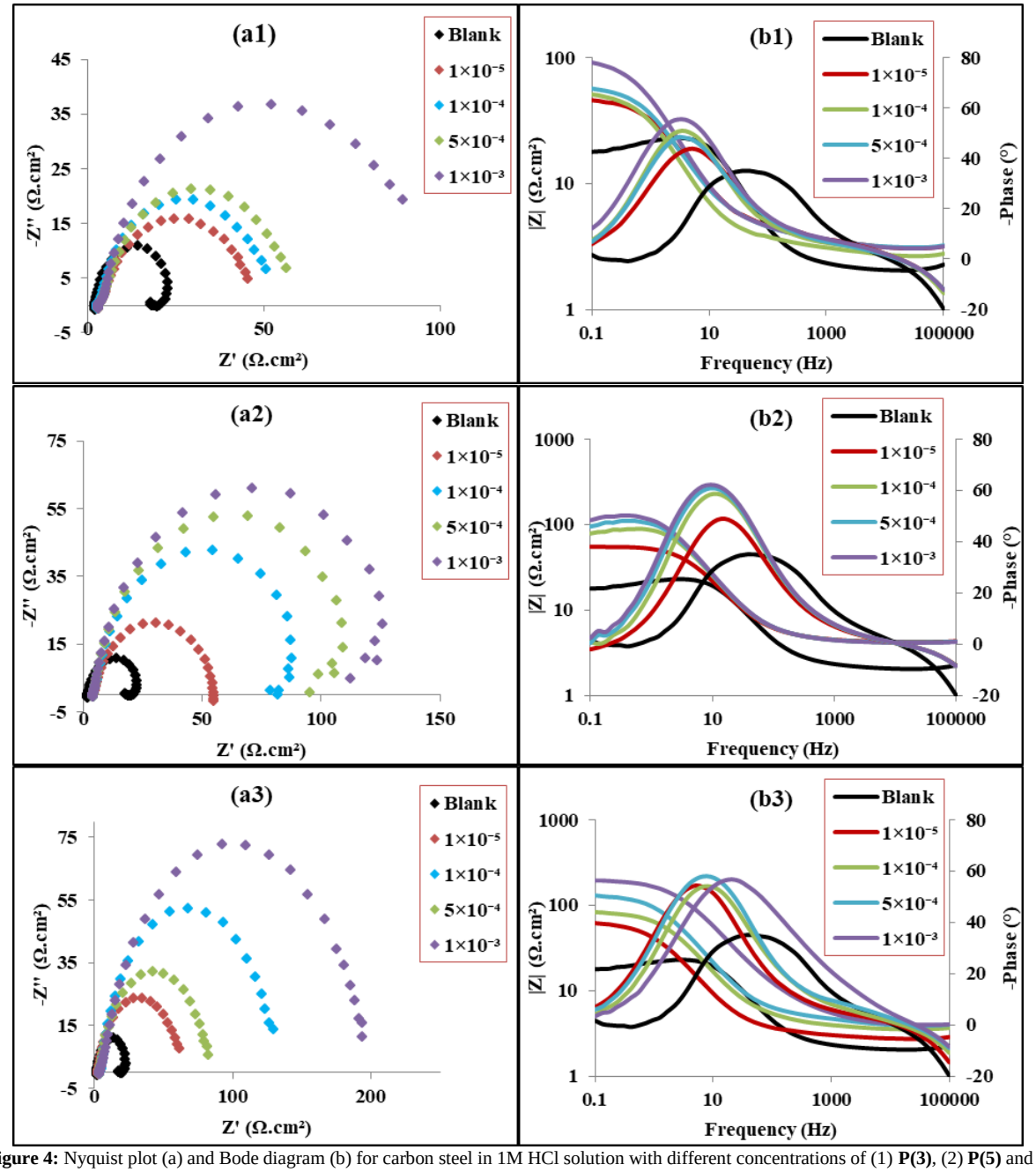

Figure 4: Nyquist plot (a) and Bode diagram (b) for carbon steel in 1M HCl solution with different concentrations of (1) **P(3)**, (2) **P(5)** and (3) **P(6)** at room temperature

3.4. Adsorption Isotherm

The Tafel-derived surface coverage values (θ) at rising pyrimidine derivatives concentrations led to best consistency with the Frumkin adsorption isotherm, with R^2 near to 1, as shown in **Figure 5**, applying the coming equation [26]:

$$log\left(\frac{\theta}{C(1-\theta)}\right) = logK + g\theta \qquad (4)$$

where K is the adsorption equilibrium constant in M^{-1} and C is the concentration of the tested pyrimidine derivatives in molarity. Equation [27] gave the standard free energy of adsorption value ($\Delta G°_{ads}$):

$$K = \frac{1}{55.5} exp\left(\frac{-\Delta G^o_{ads}}{RT}\right) \qquad (5)$$

where T the absolute temperature, R the universal gas constant, and 55.5 the water molarity. Three points are provided from **Table 4**: The first is that the synthetic chemical adsorption process is spontaneous, as evidenced by the negative values of ΔG^o_{ads} that were derived using the preceding equation. Second, since these energy levels are less than the -40 kJ/mol needed for chemical adsorption, physical adsorption is advised [28-30]. Third, the ΔG^o_{ads} values increase in the order: ***P(3)*** < ***P(5)*** < ***P(6)***, as expected from the above results.

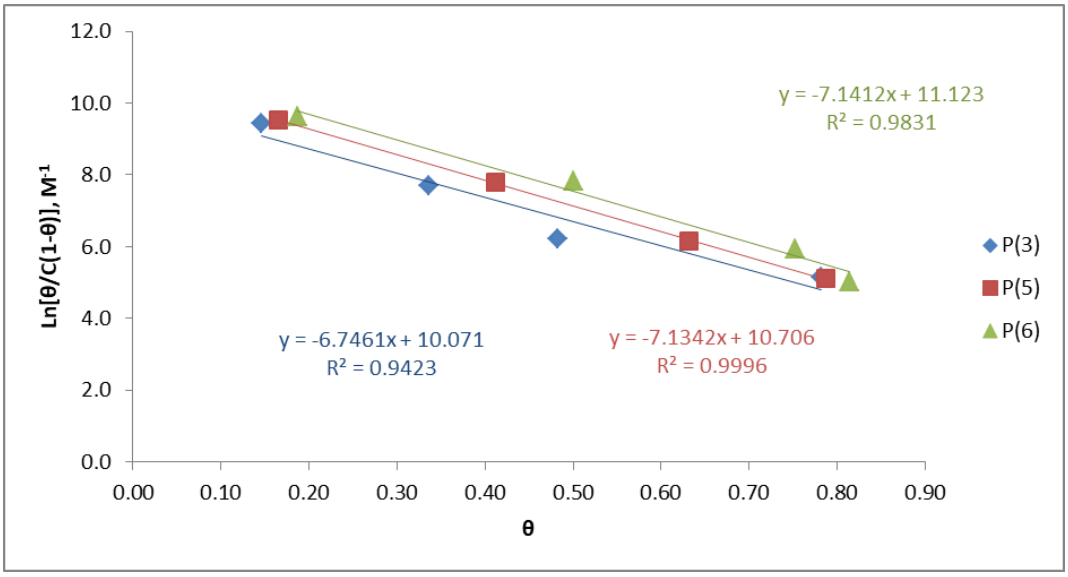

Figure 5: Frumkin adsorption isotherm for **P(3)**, **P(5)** and **P(6)** in 1M HCl solution

Table 4: The equilibrium constant of adsorption (K_{ads}) and the adsorption free energy of the inspected Pyrimidine derivatives adsorbed on the surface of carbon steel in 1M HCl at room temperature

Inhibitor	K_{ads}	ΔG_{ads} kJ/mol
P(3)	4.187	-13.502
P(5)	4.483	-13.671
P(6)	4.637	-13.755

3.5. SEM analysis:

Scanning electron microscopy (SEM) is becoming a more helpful tool for analyzing the surface morphology of both corroded and uncorroded metals. By capturing SEM pictures of the steel surface in the presence and absence of 10^{-3} M of the produced pyrimidine derivative compound ***P(6)*** in 1 M HCl solution over the course of an hour, the interactions between the studied pyrimidine derivative compound ***P(6)*** and carbon steel samples were determined. The results are shown in **Figure 6**.

The steel specimens appeared to be severely corroded and full of pits and cavities, probably as a result of the corrosive solution's aggressive attack, as **Figure 6a** shows.

The carbon steel treated with the inhibitor in the corrosive solution for an hour, however, showed

a smooth surface in the SEM image, demonstrating that the steel surface had been shielded by the inhibitor coating (**Figure 6b**).

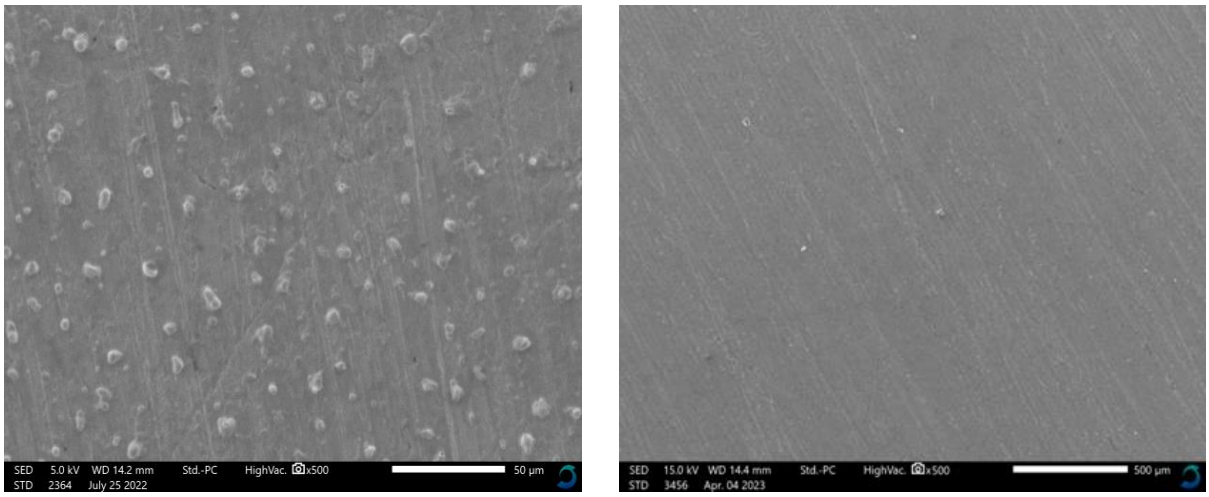

(a) **(b)**

Figure 6: SEM images for carbon steel in 1M HCl (a) without and with (b) **P(6)**

3.6. Mechanism of Inhibition

The low negative ΔG values suggest that physisorption, or the electrostatic interaction of the dipoles on the adsorbed species with the opposite electric charge of the metal surface, is most likely what causes the adsorption process [31–35].

The results showed that the electrical attraction between the pyrimidine derivatives molecules and the metal surface, which is enabled by the benzene rings' support for keeping the molecules' flat layout against the carbon steel interface, is the main driver for the size distribution and the molecules adsorption on the carbon steel interface [36-37]. The inhibition is probably due to their physical adsorption on the carbon steel surface. This occurs as a result of the adsorbed molecules' electrostatic affinity to the carbon steel interface. The formed layer slows down the metal's rate of corrosion by physically separating the metal from the aggressive acidic medium.

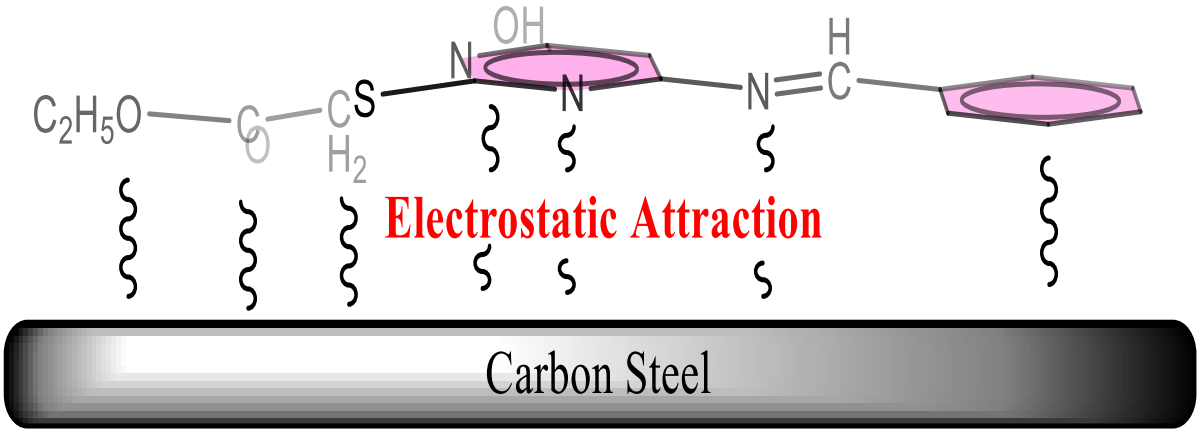

Figure 7: Adsorption of **P(6)** on carbon steel

REFERENCES

[1] SCRIVEN, E. F. V. *Comprehensive heterocyclic chemistry*. Pergamon Press, 1984.

[2] KATRITZKY, Alan R. *Advances in heterocyclic chemistry*. Academic press, 1997.

[3] DASKALOVA, Lalka I.; BINEV, Ivan. Computational study of energies and structures of 2, 4, 6-pyrimidinetrione and its anions. *International journal of quantum chemistry*, 2006, 106.6: 1338-1345.

[4] Goto, S., Tsuboi, H., Kanoda, M., Mukai, K., & Kagara, K. The process development of a novel aldose reductase inhibitor, FK366. Part 1. Improvement of discovery process and new syntheses of 1-substituted quinazolinediones. *Organic process research & development*, 2003, 7.5: 700-706.

[5] ARIZA, Xavier; BOU, Valenti; VILARRASA, Jaume. A new route to 15N-labeled, N-alkyl, and N-amino nucleosides via N-nitration of uridines and inosines. *Journal of the American Chemical Society*, 1995, 117.13: 3665-3673.

[6] CABRINI, Marina; LORENZI, Sergio; PASTORE, Tommaso. Effects of thiosulphates and sulphite ions on steel corrosion. *Corrosion Science*, 2018, 135: 158-166.

[7] PALANISAMY, Geethamani. Corrosion inhibitors. *Corrosion inhibitors*, 2019, 2019: 1-24.

[8] Kalaiselvi, K., Chung, I. M., Kim, S. H., & Prabakaran, M. Corrosion resistance of mild steel in sulphuric acid solution by Coreopsis tinctoria extract: electrochemical and surface studies. *Anti-Corrosion Methods and Materials*, 2018, 65.4: 408-416.

[9] Akbas, E., Celik, S., Ergan, E., & Levent, A. Synthesis, characterization, quantum chemical studies and electrochemical performance of new 4, 7-dihydrotetrazolo [1, 5-a] pyrimidine derivatives. *Journal of Chemical Sciences*, 2019, 131: 1-10.

[10] Kang, D., Fang, Z., Huang, B., Lu X., Zhang, H., Xu H., Huo, Z., Zhou Z., Yu, Z., Meng, Q., Wu, G., Ding, X., Tian, Y., Daelemans, D., D. Clercq, E., Pannecouque, C., Zhan, P., Liu, X. Structure-based optimization of thiophene [3, 2-d] pyrimidine derivatives as potent HIV-1 non-nucleoside reverse transcriptase inhibitors with improved potency against resistance-associated variants. *Journal of medicinal chemistry*, 2017, 60.10: 4424-4443.

[11] Sarkar, T. K., Saraswat, V., Mitra, R. K., Obot, I. B., & Yadav, M. Mitigation of corrosion in petroleum oil well/tubing steel using pyrimidines as efficient corrosion inhibitor: Experimental and theoretical investigation. *Materials Today Communications*, 2021, 26: 101862.

[12] Abdel-Raheem, S., El-Dean, A., Hassanien, R., El-Sayed, M., Sayed, M., & Abd-Ella, A. Synthesis and spectral characterization of selective pyridine compounds as bioactive agents. *Current Chemistry Letters*, 2021, 10.3: 255-260.

[13] Eid, S. Expired Desloratidine drug as inhibitor for corrosion of carbon steel pipeline in hydrochloric acid solution. *International Journal of Electrochemical Science*, 2021, 16.1: 150852.

[14] Solmaz, R., Kardaş, G. Ü. L. F. E. Z. A., Çulha, M., Yazıcı, B., & Erbil, M. E. H. M. E. T. Investigation of adsorption and inhibitive effect of 2-mercaptothiazoline on corrosion of mild steel in hydrochloric acid media. *Electrochimica Acta*, 2008, 53.20: 5941-5952.

[15] Selvam, T. P., James, C. R., Dniandev, P. V., & Valzita, S. K. A mini review of pyrimidine and fused pyrimidine marketed drugs. *Research in Pharmacy*, 2015, 2.4.

[16] Sastri, V. S. Types of corrosion inhibitor for managing corrosion in underground pipelines. *Underground Pipeline Corrosion*, 2014, 166-211.

[17] PE, P. A. S. Fundamentals of corrosion: Mechanisms, causes, and preventative methods. 2009.

[18] Fouda, A. S., Abdallah, Y. M., & Nabil, D. Dimethyl pyrimidine derivatives as corrosion inhibitors for carbon steel in hydrochloric acid solutions. *International Journal of Innovative Research in Science, Engineering and Technology*, 2014, 3.5: 12965-12982.

[19] El-Etre, A., Tantawy, A. H., Eid, S., & Seyam, D. F. Research article open access corrosion inhibition of aluminum by novel amido-amine based cationic surfactant in 0.5 M HCl solution. *Journal of Basic and Environmental Sciences*, 2017, 2: 128-139.

[20] Cristofari, G., Znini, M., Majidi, L., Bouyanzer, A., Al-Deyab, S. S., Paolini, J.,
Hammouti, B., & Costa, J. Chemical composition and anti-corrosive activity of Pulicaria mauritanica essential oil against the corrosion of mild steel in 0.5 M H2SO4. *International Journal of Electrochemical Science*, 2011, 6.12: 6699-6717.

[21] Geethamani, P., & Kasthuri, P. K. Adsorption and corrosion inhibition of mild steel in acidic media by expired pharmaceutical drug. *Cogent chemistry*, 2015, 1.1: 1091558.

[22] Ma, X., Dang, R., Gong, Y., Luo, J., Zhang, Y., Fu, J., Li, C., & Ma, Y. Electrochemical studies of expired drug (formoterol) as oilfield corrosion inhibitor for mild steel in H2SO4 media. *International Journal of Electrochemical Science*, 2020, 15.3: 1964-1981.

[23] Hernández, H. H., Reynoso, A. R., González, J. T., Morán, C. G., Hernández, J. M., Ruiz, A. M., Hernández, J. M., &

Cruz, R. O. Electrochemical impedance spectroscopy (EIS): A review study of basic aspects of the corrosion mechanism applied to steels. *Electrochemical impedance spectroscopy*, 2020, 137-144.

[24] Liangtian, Y., Zhang, M., Shidong, C., Yunji, T., & Haixia, W. Investigation of corrosion inhibition effect of enprofylline drug on mild steel corrosion in sulphuric acid solution. *International Journal of Electrochemical Science*, 2020, 15.6: 5102-5114.

[25] Fouda, A. S., Rashwaan, S., Ibrahim, H., & Ahmed, R. E. Corrosion inhibition of α-brass alloy in aqueous solution by using expired Ranitidine. *International Journal of Electrochemical Science*, 2020, 15.7: 5982-6000.

[26] Raghavendra, N. Antifebrin drug prepared via one-stage green method as sustainable corrosion inhibitor for Al in 3 M HCl medium: insight from electrochemical, gasometric, and quantum chemical studies. *Surface Engineering and Applied Electrochemistry*, 2020, 56.2: 235-241.

[27] Milonjić, S. K. A consideration of the correct calculation of thermodynamic parameters of adsorption. *Journal of the Serbian chemical society*, 2007, 72.12: 1363-1367.

[28] Hamdy, A., & El-Gendy, N. S. Thermodynamic, adsorption and electrochemical studies for corrosion inhibition of carbon steel by henna extract in acid medium. *Egyptian Journal of Petroleum*, 2013, 22.1: 17-25.

[29] Vaszilcsin, N., Duca, D. A., Flueraş, A., & DANa, M. L. Expired drugs as inhibitors in electrochemical processes–a mini-review. *Stud. Univ. Babes-Bolyai Chem*, 2019, 64.3: 17-32.

[30] Kooliyat, R., Kakkassery, J. T., Raphael, V. P., Cheruvathur, S. V., & Paulson, B. M. Synthesis, Cyclic Voltammetric, Electrochemical, and Gravimetric Corrosion Inhibition Investigations of Schiff Base Derived from 5, 5-Dimethyl-1, 3-cyclohexanedione and 2-Aminophenol on Mild Steel in 1 M HCl and 0.5 M H2SO4. *International Journal of Electrochemistry*, 2019, 2019.1: 1094148.

[31] Farhadian, A., Rahimi, A., Safaei, N., Shaabani, A., Abdouss, M., & Alavi, A. A theoretical and experimental study of castor oil-based inhibitor for corrosion inhibition of mild steel in acidic medium at elevated temperatures. *Corrosion Science*, 2020, 175: 108871.

[32] Ituen, E. B., & Udo, U. E. Phytochemical profile, adsorptive and inhibitive behaviour of Costus afer extracts on aluminium corrosion in hydrochloric acid. 2012.

[33] Abdallah, M., Kamar, E. M., Eid, S., & El-Etre, A. Y. Animal glue as green inhibitor for corrosion of aluminum and aluminum-silicon alloys in sodium hydroxide solutions. *Journal of Molecular Liquids*, 2016, 220: 755-761.

[34] Khadraoui, A., Khelifa, A., Touafri, L., Hamitouche, H., & Mehdaoui, R. Acid extract of Mentha pulegium as a potential inhibitor for corrosion of 2024 aluminum alloy in 1 M HCl solution. *J. Mater. Environ. Sci*, 2013, 4.5: 663-670.

[35] Seyam, D. F., H. Tantawy, A., Eid, S., & El-Etre, A. Y. Study of the inhibition effect of two novel synthesized amido-amine-based cationic surfactants on aluminum corrosion in 0.5 M HCl solution. *Journal of Surfactants and Detergents*, 2022, 25.1: 133-143.

[36] Elsaoud, A. A., Mabrouk, E. M., Seyam, D. F., & El-Etre, A. Recyclization of expired Megavit Zinc (MZ) drug as metallic corrosion inhibitor for copper alloy C10100 in nitric acid solution. *Journal of Bio-and Tribo-Corrosion*, 2021, 7: 1-9.

[37] Seyam, D. F., Eid, S., & Tantawy, A. H. Study the Inhibition effect of Three Newly Synthesized Schiff Base Based Cationic Surfactants on Aluminum Corrosion in 0.5 M HCl Solution. *Egyptian Journal of Chemistry*, 2023, 66.4: 87-99.

[38] Felaly, R. N., Alfakeer, M., Ali, A. A., Al-Juaid, S. S., Mabrouk, E. M., El-Etre, A. Y., Seyam, D. F., & Abdallah, M. Enhanced corrosion protection of copper alloy in 2.0 M HNO3 solution using expired solo sept, slim-lax and well derm drugs. *International Journal of Electrochemical Science*, 2024, 100657.